

POLITECNICO DI MILANO



PhD Yearbook | 2008

PHYSICS

Index

A

Antognazza, Maria Rosa 6

B

Benedetti, Enrico 8

Brambilla, Marco 10

Brenna, Massimiliano 12

C

Cattoni, Andrea 14

Celebrano, Michele 16

Chiodo, Nicola 18

Coluccelli, Nicola 20

F

Ferrari, Raffaele 22

G

Gatti, Davide 24

O

Osmond, Johann 26

P

Piazzalunga, Andrea 28



Chair:
Prof. Franco Ciccacci

DOCTORAL PROGRAM IN PHYSICS

The Doctoral Program in Physics at Politecnico di Milano aims to attract bright students with good scientific background and marked interest towards development and applications of new ideas and technologies. It offers a wide range of opportunities in the fields of advanced applied physics, such as photonics and optoelectronics (lasers, optical disks, optical communications), vacuum technologies (thin film depositions), material technologies (microelectronics and nanotechnologies, micromechanical processing), advanced instrumentation (electronic and atomic microscopy, nuclear magnetic resonance) and biomedical optics (optical tomography).

The PhD course is characterized by a strong experimental character. Its main purpose is the development of an experimental approach in problem solving techniques and the attainment of a high level of professional qualification. Scientific education and training to develop general research abilities in all areas of applied physics is increasingly needed by advanced technological industries. The PhD program aims at providing engineers and physicists, after a Bachelor of Science ("Laurea", 3 years) and a Master of Science ("Laurea Magistrale", 2 years), with a general education in the basic areas of applied physics and a specific knowledge in condensed matter physics, optics and lasers.

The contents of the doctoral program are strictly related to the research activities carried out in the laboratories at the Department of Physics. They can be divided into two main areas:

- Condensed Matter Physics, including photoemission; spin-resolved electronic spectroscopy; magneto-optics; X ray diffraction; magnetic nanostructures for spintronics; synchrotron radiation spectroscopy, positron spectroscopy, semiconductor nanostructures.
- Optics and Quantum Electronics, including biomedical applications of lasers, laser applications in optical communications; diagnostics for works of art; time-resolved optical spectroscopy; ultrashort light pulse generation and applications; UV and X optical harmonics generation.

All these research activities make use of advanced experimental laboratories located at Politecnico di Milano (Milano-Leonardo Campus and Como Campus) and are performed in collaboration with several international Institutions. Besides the experimental research, a consistent effort is devoted to the design and development of novel instrumentation.

As for the educational program, it can be divided into four parts: 1) Laboratory of Basic Physics, implying that the students join full time different experimental laboratories, guided by their tutor as well as other colleagues at the Department of Physics; 2) Main courses specifically designed for the PhD program; 3) activities pertaining more specific disciplines which will constitute the basis of the research work to be carried out during the Doctoral Thesis; 4) Doctoral Thesis. The thesis work (which constitutes the most relevant part of the program) has a marked experimental character and will be carried out in one or more laboratories at the Department of Physics. Based on the scientific collaborations of the Department, the students are encouraged to perform their thesis work also in laboratories of other national or foreign Institutions. Numerous collaborations, which the PhD students may be involved in, are presently active with several national and international Institutions, such as: ETH-Zürich, EPL-Lausanne, Lund Institute of Technology, University of Paris-sud, Ecole Polytechnique-Paris, University of Barcelona, University of Berkeley, Technical University of Wien,

University of Bordeaux, MIT-Cambridge, INFN-CNR, IIT-Istituto Italiano di Tecnologia, European Space Agency, ENEA, Elettra-Ts, PSI-Villigen, Agenzia Spaziale Italiana, European Synchrotron Radiation Facility (ESRF-Grenoble).

The mean number of fellowship-grants for students entering the PhD program is around eight per year, while the mean number of available positions is sixteen per year. At present the overall number of students in the three-years course is thirty.

Teaching and research activities of the Doctoral Program are controlled and organized by a number of Faculty members large enough to cover a wide spectrum of research fields. All members are highly qualified and active researchers. This ensures a continuous updating of the PhD program and guarantees that the students are involved in innovative work.

The Doctoral Program relies also upon a Steering Committee, formed by distinguished experts (see table below) coming from R&D industries or Research Labs, taking care that the goals of the PhD program conform with the needs of non academic world.

DOCTORAL PROGRAM BOARD

Lucio Braicovich	Lamberto Duò	Orazio Svelto
Giulio Cerullo	Alfredo Dupasquier	Paola Taroni
Franco Ciccacci	Paolo Laporta	Hans Von Kaenel
Rinaldo Cubeddu	Ezio Puppini	
Sandro De Silvestri	Roberta Ramponi	

ADVISORY BOARD

Gianfranco Canti (Dipartimento di Farmacologia, Università di Milano)	Ubaldo Mastromatteo (ST Microelectronics)
Marco Fanciulli (INFN-CNR)	Marco Romagnoli (Pirelli Labs)
Bruno Ferrario (SAES - Getter Spa)	

SCHOLARSHIP SPONSORS

Italian Institute of Technology (IIT)
Italian Ministry for University and Research (MIUR)
National Institute for the Physics of Matter - National Council for Research (INFN-CNR)
SAES-Getters Spa

PHOTOPHYSICS AND APPLICATION OF ORGANIC SEMICONDUCTORS FOR ARTIFICIAL VISION

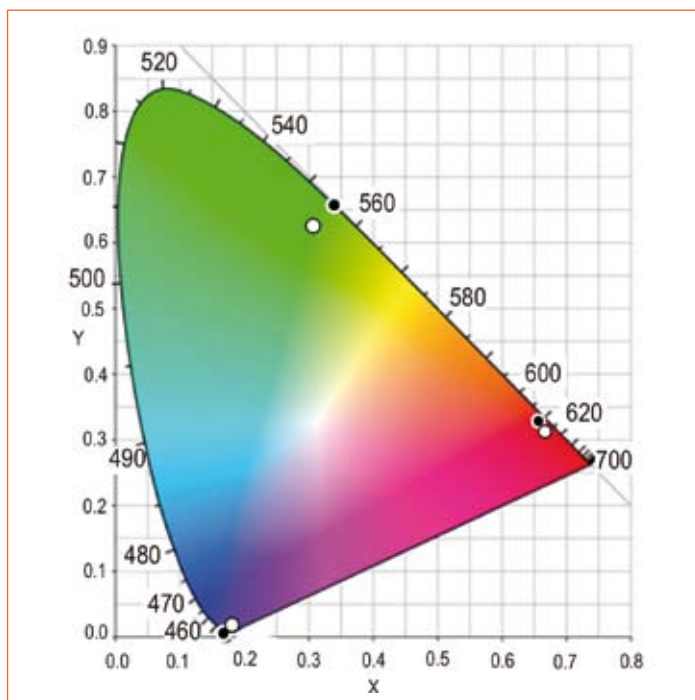
Maria Rosa Antognazza

My activity has been focused onto two major objectives: (a) the realization of a color sensor based on conjugated, organic materials, working in a tristimulus approach, and (b) the fundamental study of the main photophysical processes involved in the vision process.

a. The first step of the work consisted in properly selecting three active, organic materials whose photocurrent spectral responsivity could reproduce the color matching functions of a standard observer and/or the spectral response of the photoreceptors naturally present in our retina. After that, using the most appropriate materials, we realized a system of three photodiodes, exploitable as a color sensor.

The performances of the device, in terms of efficiency and measurement precision, were directly tested for some color stimuli, as reported in [Fig. 1]. The results demonstrated the feasibility of the approach, and paved the way for further exploitation of organic semiconductors both for colorimetric applications and for artificial retina.

The research followed two different, complementary ways: we focused onto the possible, practical applications of the color sensor, trying to improve the performances of the devices. The final aim was the

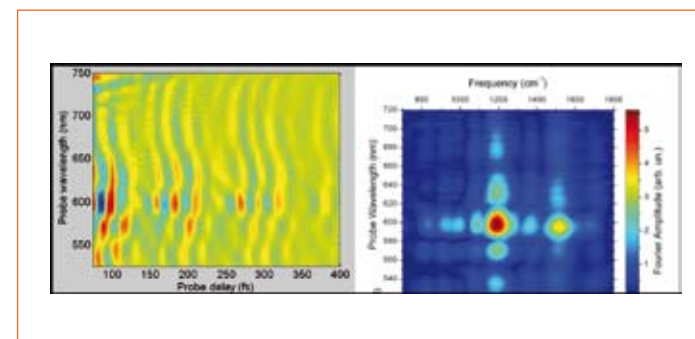


1. The chromaticity coordinates provided by the organic colorimeter for three test-stimuli (solid circles), compared with the standard observer ones (open circles)

integration of the organic color sensor in an already existing, commercial colorimeter; the optimization process, even if not yet completed, is providing promising results.

A preliminary study investigated the possibility of using organic semiconductors technology for artificial vision applications, namely in robotics and biologic applications. We studied the effect of the contact with water (which

can not be disregarded in a biological environment) onto the photophysical properties of some prototype polymers and we also realized a new generation of photodiodes, using as a cathode some ionic solutions, commonly used in cell culturing protocols. We demonstrated in this way the possibility to grow some neural networks directly in contact with polymers. We also designed an array of



2. Photoexcitation dynamics in a model system, similar to the retinal, in the time and the frequency domain. It is possible to monitor the molecular oscillations in real time

organic photodiodes, with a geometric arrangement reproducing the natural one. Finally, we investigated the effect of the discrepancy between the spectral responses of the natural and the artificial photoreceptors; the issue is strongly related to the mechanism of colour constancy.

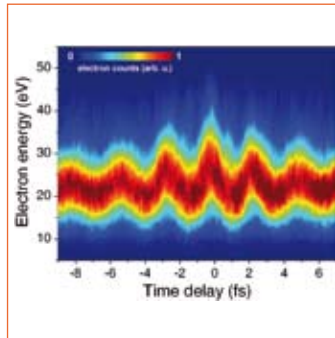
A parallel work aimed at understanding the mechanism of vision on a molecular level. The properties of a long chain polyene, belonging to the same family of retinal and very similar to it, were investigated. We made use of time-resolved spectroscopy techniques with extreme temporal resolution, up to femtosecond timescales [Fig. 2], and other spectroscopic techniques, namely cw-photoinduced absorption, electroabsorption, charge

induced spectroscopy. More in detail, our attention was focused on the formation mechanisms of the triplet states, which play very important roles in defending our organism (and specially our retina) against oxidation and photodegradation. It was put in evidence that triplets are formed in correlated pairs by a peculiar process, known as ultrafast singlet fission. This result might help to clarify the earliest processes involved in vision, and to understand which way human retina protects itself.

ATTOSECOND PULSES: GENERATION, CHARACTERIZATION AND APPLICATION TO ELECTRON WAVEPACKET IMAGING

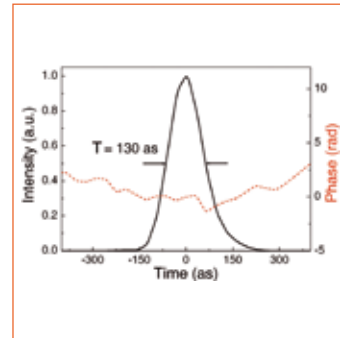
Enrico Benedetti

In the last few years dramatic progress has been achieved in the field of attosecond technology ($1 \text{ as} = 10^{-18} \text{ s}$). This headway is mainly due to breakthroughs in laser science and to the introduction of new techniques for temporal characterization of eXtreme UltraViolet (XUV) attosecond pulses. Attosecond science is now a well-established research field, which promises to offer formidable tools for the investigation and control of fundamental atomic and subatomic electron processes. The duration of a light pulse is limited by the period of the optical cycle. Therefore, the generation of attosecond pulses requires employing XUV radiation. The XUV light pulses are produced exploiting the process of High order Harmonic Generation (HHG) in gas by an InfraRed (IR) laser pulse (5 fs, 300 μJ @ 800 nm). The HHG process can be essentially understood in the framework of a semi-classical model. Consider an atom of gas and its outermost electron. Focusing the laser field (10^{14} W/cm^2) on the gas, the Coulomb potential of atom is deformed: by tunnelling ionization the electron can escape in the continuum. Subsequently, the electron accelerates away from the atom until the field changes sign.



1. Experimental FROG CRAB trace: it shows the electron energy spectrum evolution as a function of time delay between XUV and IR pulses. The energy shift of electron versus the time delay represents the vector potential of IR field

Depending on the phase of IR field at the ionization instant, the electron can revisit and recombine with the parent ion. In this case a photon with frequency $\omega = (I_p + E_k)/h$ is emitted, where E_k indicates the kinetics energy gained by the electron in the continuum and I_p is the ionization potential of neutral atom. As the process is repeated twice per laser cycle, in the time domain the emitted radiation is equivalent to a train of attosecond pulses and in the spectral domain to a spectrum composed by several odd harmonics, extending well into the XUV region. HHG produces an attosecond pulses train, but for a number of important applications isolated attosecond pulses are required. In order to



2. Reconstruction of the temporal intensity profile and phase of the attosecond pulses obtained from the FROG CRAB trace shown in [Fig. 1]. The attosecond pulse was generated in Argon

achieve this aim, we need to limit the HHG generation to a half-cycle of the laser field. The HHG process is strongly sensitive on the ellipticity of the IR field. The HHG efficiency is maximum when the ellipticity is zero (linear polarization) and decreases quickly as the ellipticity increases. Typically a 10-15% ellipticity reduces the generation efficiency by a factor of two. Carrying out HHG with an IR pulse that is only linearly polarized for a short time (and elliptically polarized elsewhere) ensures that the XUV emission is temporally confined inside a "polarization gate", where the fundamental ellipticity is small. This way to select an isolated attosecond pulse is called polarization gating technique.

To modulate the laser pulse polarization, we have used a simple technique based on the use of two birefringent quartz plates, achieving both a rapid modulation of the ellipticity and a 100% transmission of the input pulse energy. We stress that this technique requires short laser pulses ($< 7 \text{ fs}$) with stable carrier-envelope phase. Polarization gating technique allows one the production of ultra-broadband and tunable continuous spectra. The generation efficiency is around 10^{-7} for Argon and $5 \cdot 10^{-9}$ for Neon. Complete temporal characterization of the attosecond pulses has been obtained using for the first time the technique of Frequency Resolved Optical Gating for Complete Reconstruction of Attosecond Burst (FROG CRAB). The XUV attosecond pulse ionizes a gas (Argon), by single photon absorption, thus generating an attosecond electron pulse, which, far from any resonance, is a perfect replica of the optical pulse. Direct information on temporal structure of XUV pulse can thus be obtained by characterizing the electron wavepacket. The conversion of the XUV pulse into an electron wavepacket is obtained in the presence of a IR pulse, whose electric field acts as an ultrafast phase

modulator on the generated electron wavepacket. In this way, a time-nonstationary filter, which is required to achieve the temporal characterization of the ultra-short pulse, is realized. The evolution of the photo-ionization spectra as a function of the delay between the XUV and the IR pulses, the FROG CRAB trace, allows one to retrieve the temporal intensity profile and phase of the XUV pulses and the electric field of the IR pulse. [Fig. 1] shows a FROG CRAB trace and [Fig. 2] shows the corresponding retrieved XUV pulse: with a duration as short as 130 as, which consist of less than 1.2 periods of the central frequency (around 36 eV photon energy), this is the shortest light pulse created so far. We have then generated attosecond pulses in Xenon gas, with a spectral bandwidth broad enough to excite coherently the entire discrete spectrum with angular momentum $\ell=1$ in Helium and part of the continuum spectrum. The created wavepackets are analyzed by using an ultra-short IR laser field to ionize the excited wavepacket. The wavepacket ionized directly by XUV pulse and the wavepacket ionized by XUV and IR pulses interfere. By finely varying the delay between the XUV and IR pulses, information can be deduced

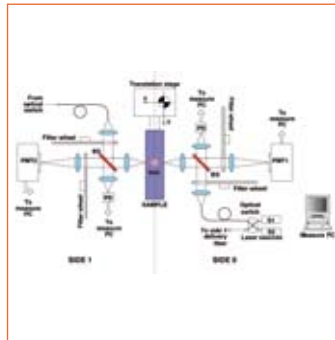
on the dynamics of the created wavepackets (the analysis of these data is still in progress). The availability of few-cycle isolated pulses in the photon energy range of about 30 eV is particularly important for the study of electron dynamics in chemistry and molecular and solid state physics, in which a number of fundamental processes are related to the outermost electrons, directly accessible by the generated attosecond pulses. On the other hand, the possibility of generating single-cycle pulses of less than 100 as at higher energy with the use of the polarization gating method in Neon should allow the study of the coherent dynamics of inner-shell electrons with unprecedented temporal resolution. Thus, the recent progresses in the attosecond technology, that are presented in this work, open up a new regime for time resolved tomography of atomic or molecular wavefunctions and ultrafast dynamics.

FLUORESCENCE MOLECULAR IMAGING IN THE TIME DOMAIN

Marco Brambilla

Molecular imaging is a family of many different diagnostic techniques aimed at the localization, and possibly the quantification, of suitable markers inside the body of a living subject. What is particularly attractive, is the possibility not only to study a given biological phenomenon at a certain stage of its development, but to follow its evolution directly, in vivo and on the same individual.

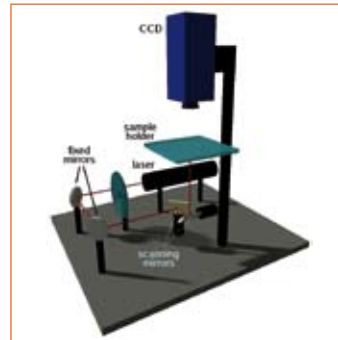
Recently, beside "classical" molecular imaging techniques such as functional magnetic resonance imaging (fMRI), positron emission tomography (PET) or single photon emission tomography (SPECT), optical molecular imaging is emerging as one of the most attractive, given its great advantages over nuclear modalities. Optical molecular imaging is in fact based on the detection of fluorescent light in the visible-near infrared region of the electromagnetic spectrum: this implies involving no ionizing radiation and using fluorescent dyes as contrast agents, whose cost, availability and handling are far more convenient than nuclear or magnetic ones. The greatest poser optical molecular imaging has to face is the fact that biological tissues are not optically transparent media. Light propagating through them is subject to



1. Time resolved scanning system scheme

a wavelength dependent attenuation and strong diffusion. The scattering is a big issue (probably the biggest), because if attenuation limits the possibility to investigate deeper regions, diffusion imposes a big limitation on achievable resolution.

To take into account these phenomena, mathematical models of light propagation in highly diffusive media have been studied since 1970. Presently, the most popular model of light diffusion is the, which is an approximate model originally developed to describe the transport of neutrons in nuclear applications. It can accurately describe how photons diffuse in highly scattering media, taking into account also phenomena like fluorescence, which is the contrast enhancing physical process involved with optical molecular imaging.



2. Continuous wave CCD based system scheme

Even though it is a complex phenomenon, fluorescence is commonly approximating as a two-states quantum process, during which a fluorophore molecule is excited at a single wavelength (*the excitation wavelength*), remains in the excited state for a certain amount of time (*the fluorescence lifetime*, few nanoseconds) and returns to its fundamental state, emitting a photon at a single wavelength (*the emission wavelength*) slightly longer than the excitation one (Stokes's shift). To detect a fluorescent inclusion inside a diffusing sample some sort of excitation light must therefore be delivered to it, and light emitted by the dye must be discriminated by the excitation one: this can be achieved by means of convenient optical filters placed in front of the optical detector.

During the doctoral period two different optical molecular imaging systems for small animals have been developed and have been tested and fully characterized on tissue-simulating phantoms with point fluorescent inclusions embedded.

The first one exploits the time correlated single photon counting technique, which allows the detection of the intensity of a light pulse as short as few hundreds picoseconds as function of time. Analyzing the changes of the pulse shape after it had traveled through a diffusive medium, it is possible to recover many informations about the optical properties of the sample and the intensity and the lifetime of eventual fluorescence sources present in the medium.

The system is depicted in figure 1. It is a scanning system capable of simultaneously detecting transmitted and back-scattered light from both sides of the sample. By means of free air optical stages, excitation pulses produced by a pulsed laser diode are injected into the sample and stimulate fluorescence. Emitted light is collected and delivered to the photomultiplier tubes by means of the same optics. A flexible filter management assembling allows injected and collected light wavelengths selection.

The characterization has been carried out by measuring various phantoms, each differing from one another by optical properties, fluorophore concentration inside the inclusion or inclusion position. The system has shown a good linearity in detecting optical parameters of the phantoms, and a very good linearity also against the fluorophore concentration inside the inclusion. Moreover, given the 'on-axis' configuration of the injection and detection stages, transmittance data have turned out to be insensitive to inclusion depth.

The second system is sketched in figure 2. It is a CW system, based on CCD camera detection for transmittance imaging only. To excite the fluorescent sources inside the whole sample, all its surface is illuminated by raster scanning the beam of a CW Helium-Neon laser on the injection surface for all the duration of the CCD acquisition. The system has been tested and characterized on phantoms: being a CW system, optical properties cannot be any more recovered and only linearity against inclusion concentration has been validated with satisfying results. Since with this configuration data are acquired in all the collection points (CCD pixels) simultaneously and with a wide area illumination, in

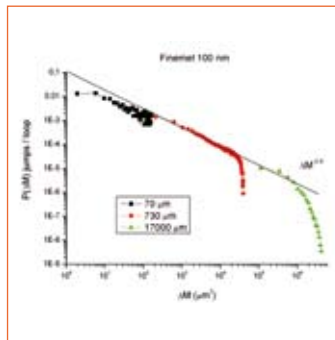
the resulting image inclusion brightness is no more depth independent. Therefore the effects of sample optical inhomogeneities and variable thickness were assessed. It turned out that fluorescence images of inhomogeneous samples contain strong artifacts, but acquiring in a second measurement the transmitted excitation light and dividing the fluorescence image by the excitation one, artifacts correction is good.

To conclude, the realization and characterization of these two systems has given the possibility to compare the actually most popular optical molecular imaging techniques and to investigate the contribution of time information: it turned out that for planar imaging scanning transmittance is superior, even if it requires more complex experimental setup and measurement procedures, while CCD detection is more performing for tomographic data acquisition. Time information is not a critical information for fluorescence intensity estimation, but it becomes essential for the recovery of optical properties of the sample, needed for accurately model light diffusion for tomographic reconstruction.

MAGNETO OPTICAL MEASUREMENTS ON THIN FERROMAGNETIC FILM

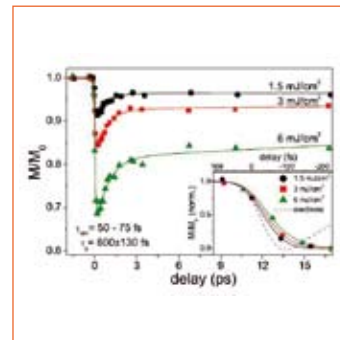
Massimiliano Brenna

During my doctorate term, I have worked in the magneto optical laboratory of the Physics Department of Politecnico di Milano, directed by Prof. Ezio Puppin. I was employed in an activity of strong experimental character. The research work that I have done has covered different side of thin film magnetism investigated by means of magneto optical techniques. The principal activity of this laboratory is the measurements of Barkhausen noise in ferromagnetic materials. The magnetization process in ferromagnetic materials is described by the well know magnetic hysteresis cycle in which the magnetization M is plotted against the applied field H . The phenomenon of hysteresis at microscopic level is strictly connected with the concept of magnetic domains and their dynamics. A magnetic sample is organized in a series of different region of space, called magnetic domains, wherein the magnetization is directed along a particular direction. During the magnetization process in a sample, we have a modification of this domain structure that is the cause of Barkhausen noise. The hysteresis curve is not continuous and regular but if measured with high resolution one can see sudden and irregular increment of the magnetization M , that



1. Histogram of Barkhausen jumps in Finemet thin film

is called Barkhausen jumps. Measuring thousand of cycles it is possible to make a statistical characterization of the intensity of these jumps respect to the overall magnetization. This phenomenon obeys to a statistical distribution of jumps amplitude that follows a power law statistics. The probability that one jump with intensity ΔM occurs is equal to $\Delta M^{-\alpha}$. The exponent α is called critical exponent. The object of the Barkhausen noise measurements is to extract the value of the critical exponent α . [Fig. 1] shows the measured histogram of intensity of Barkhausen jumps in thin Finemet film for different value of the laser spot size. In order to make this kind of measurements I have first projected some instrumental apparatus necessary to make different magneto-optical measurements on thin magnetic



2. The ultrafast transient magnetization in a thin iron film

films. I have projected and designed a head for a cryostat (helium cooled), equipped by an electromagnet. With this instrument it is possible to make measurements of hysteresis cycle at different temperatures (from 400 K down to 10 K) and with relatively strong magnetic field applied (1000 – 2000 Gauss). I have measured and analyzed the behaviour of the critical exponent in the power laws that describe the Barkhausen noise in thin films of Finemet (Fe-Si alloy) of different thickness. The results were that the value of the critical exponent depends of the thickness of the film. Another research project was that of the study of paramagnetism in thin ferromagnetic film of Fe/ZnSe interface. This system is an example of a magnetic-semiconductor system for spintronic devices. These kinds of disposal are good promises

to realize magneto electronic integration, for example MRAM (Magnetic Random Access Memory), SFET (Spin Field Effect Transistors). In that disposal we have both the capacity of elaboration and processing of the information and the storage of large amount of data. In this device is strictly necessary having a spin polarized current injected into the semiconductors. So it is necessary that a traditional semiconductors like Si or GaAs in coupled with a ferromagnetic thin film for controlling the spin state of the carriers. If the ferromagnetic film deposited onto then semiconductor is very low it is possible that there is a loss of ferromagnetism (and than the loss of the possibility of control the spin of the carriers injected into the semiconductor). I have measured many different thickness for Fe deposited onto ZnSe (semiconductor). I have found that for low value of thickness of iron the ferromagnetism was absent and the system is paramagnetic. The critical value of the thickness at room temperature was about four-six monolayer of iron deposited (one monolayer in equal to 1.5 Angstroms). Successively I have made a research on than anomalous behaviour in aromatic substances, in particular in anthracene, $C_{14}H_{10}$. In particular, the goal of the research was

that to verify the existence of a permanent magnetic dipole in these substances. If it was true it well be extremely important because aromatic substances are made only by carbon and hydrogen and so they are not ferromagnetic buu behaves like its. We have demonstrated that this effect is caused by ferromagnetic impurity included in the aromatic substances. The last argument of my thesis was the implementation of TR-MOKE experiments (Time Resolved Magneto Optical Kerr Effect) in the ULTRAS laboratory of the Physics Department. With this special technique, it is possible to make the measurement of the dynamics of the magnetization that follows a laser pulse excitation with extreme temporal resolution. This is possible by a pulsed laser source (we use a laser pulsed with a duration of one pulse about 50 femtosecond) and the pump/probe optical technique. With this extreme temporal resolution, it is possible to investigate the transitory of the magnetization on an ultra short timescale down to few hundreds of femtoseconds, see [Fig. 2]. There is a rapid drop of the magnetization during the first hundreds of femtoseconds. The study of the dynamics of magnetization on this time scale is of crucial importance not only for a pure physical interpretation

but also for a technological point of view in connession with the magneto-optical reading of information stored in magnetic disposal.

MAGNETIC TUNNELLING JUNCTIONS BASED ON MGO BARRIERS: FROM THE STUDY OF THE INTERFACES TO THE REALIZATION OF DEVICES

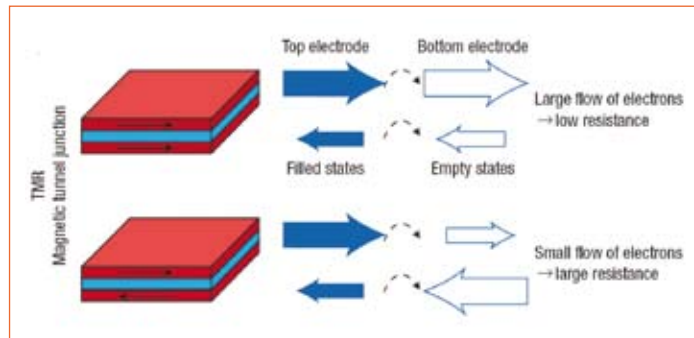
Andrea Cattoni

A Magnetic tunnelling junctions (MTJ) consists of two ferromagnetic layers (red) separated by an insulating spacer (blue) [Fig. 1]. For a sufficiently thin spacer (about 2 nm), a tunnel current can flow between the ferromagnets. Because spin is conserved in the tunnelling process, the current is larger for parallel than for antiparallel magnetizations of the two ferromagnetic layers, i.e., the resistance is lower for parallel than for antiparallel magnetizations. The factor of merit of a MTJ is the Tunneling Magneto Resistance (TMR) ratio:

$$TMR = \frac{R_A - R_P}{R_P}$$

where R_A (R_P) are the antiparallel (parallel) tunnelling resistances. Application: magnetic random access memory (MRAM), magnetic sensor.

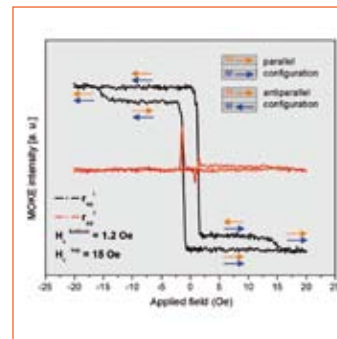
In a fully epitaxial MTJ, the TMR value is affected by the crystal quality of the ferromagnetic layers (FM) and the barrier (B), and the control on the magnetic and electrical properties of the FM/MgO interfaces is fundamental to obtain high TMR values. So far, best TMR values were obtained on MTJs based on MgO barriers [Yuasa et al., Nature Materials 3



1.

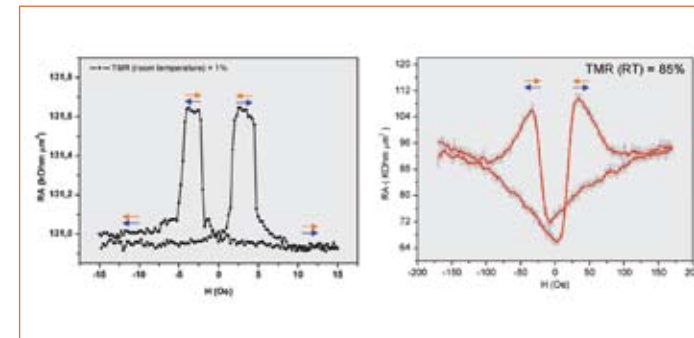
868 (2004) – Yuasa et al., App. Phys. Lett **89**, 42505 (2006)]. I performed a comparative study on the critical FM/MgO interfaces (FM= Fe(100), Fe(100)-p(1x1)O, FeCo(100)), and I realized MTJs by using shadow masks.

FM/MgO interfaces were grown by molecular beam epitaxy and analysed by means of different spectroscopic and magnetic techniques. The Fe(100)-p(1x1)O surface resulted the most stable and promising to realize good MTJs. The MTJ growth process was carried forward with the second FM layer and with the control of the coercive fields of the two FM or electrodes. Figure 2 shows a Magneto Optical Kerr Effect performed on a trilayer structure: the antiparallel configuration is achieved for applied magnetic field ranging to [-150e ÷ -0.60e] and [0.60e ÷ 150e].



2.

I-V and TMR measurements were performed on complete heterostructure: Fe(100)/Fe(100)-p(1x1)O/MgO/Fe(100) realized with different MgO thickness (3.4nm ÷ 5nm) and different junction area (0,2mm × 0,2mm and 2 × 2mm). Figure 3 shows the junction resistance as a function of the applied field: in antiparallel configuration the junction resistance is higher than in



3.

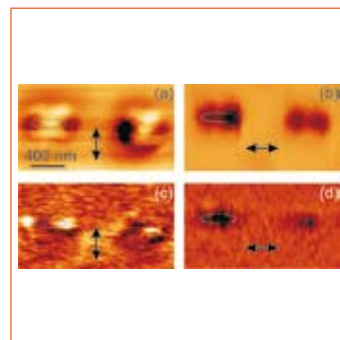
the parallel configuration. The higher TMR value obtained at room temperature was 85% (literature value 180% by Yuasa et al. on the same structure). Work in progress: nanofabrication of MTJs by using optical lithography and ion milling technique to define heterostructure with an area ranging from 5µm to 100 µm.

NEAR- AND FAR-FIELD IMAGING AND SPECTROSCOPY OF SINGLE NANOPARTICLES

Michele Celebrano

The explosive growth of nanoscience and nanotechnology in the last decade calls for a deeper understanding of light-matter interaction at the nanoscale. The wave nature of light prevents its focusing to spot sizes significantly smaller than the wavelength, providing a fundamental limit both to high-resolution optical imaging (the so-called diffraction limit) and to the engineering of mesoscopic optical circuits and devices. Nano-optics is a new rising field in physics that tries to overcome these limitations by addressing two main issues: (i) efficient coupling of light with nanoobjects (e.g. metal and semiconductor nanoparticle); (ii) tight spatial confinement of light by squeezing it into sub-diffraction limited spots. A fulfilment of the first issue would enable to guide and interface light at the nanoscale in a way to let it “communicate” with single optical q-bits and to allow for fast and efficient information transport in nanoscale optical circuits. On the other hand, light confinement is one of the obvious requirements in the development of high-resolution microscopy techniques which are strongly demanded to study chemical and physical properties of single nanostructures themselves. Indeed, a tightly focussed source

of light efficiently couples with nanoscale objects because it better matches their effective optical interacting area (cross-section). Scanning Optical Microscopy (SOM) experienced a continuous evolution through the last century; however, only in the last decades it was able to overcome the diffraction barrier by squeezing the light into sub-wavelength spots. A first step towards a better spatial resolution was done with the development of Scanning Confocal Optical Microscopy (SCOM); this technique allows to obtain a diffraction limited resolution ($\sim \lambda/2$). For the visible light, SCOM resolving power can be ~ 200 nm. Almost simultaneous was the first demonstration of scanning near-field optical microscopy (SNOM) which allows beating the diffraction limit by illuminating the sample with a nanometer-sized aperture (or a scatterer) brought in its vicinity (near field). In particular, in the aperture-SNOM light is transmitted by subwavelength hollow probe which is brought in close proximity to the sample, thus ensuring an optical resolution basically of the order of the aperture diameter (typically, 50-100 nm). During my PhD activity both SCOM and SNOM techniques were implemented for



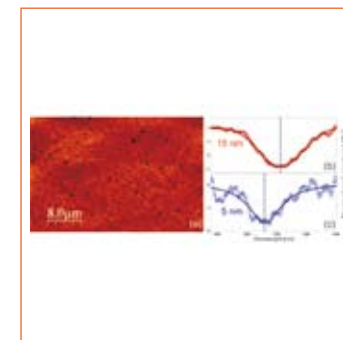
1. Gold nanoellipsoids. (a) and (b) SNOM extinction maps of 400-nm long particles obtained with cross-polarized light. (c) and (d) SHG maps from the same area. Ellipses on the left depict particles position. Arrows indicate polarization of impinging light

spectroscopy and imaging of isolated resonant metal nanoparticles and single semiconductor quantum dots. I spent the first two years in the Laboratories for Ultrafast Spectroscopy in Politecnico. During my activity in the group of Prof. De Silvestri and under the supervision of Prof. Cerullo, I have developed an aperture SNOM system coupled with a femtosecond laser source, in order to induce nonlinear effects at the nanoscale. This system preserves pulse duration and polarization through the aperture, allowing for a strong spatial confinement of high peak-power pulses. In collaboration with the Suspenx group in the Physics

Department, we used the setup to image the nonlinear optical response of elliptical gold nanoparticles (with variable lengths from 100 to 400 nm) by detecting second harmonic generation (SHG) in the near field. As an example, Fig. 1 shows simultaneously acquired extinction and SHG maps of gold nanoellipsoids which display different spatial response with respect to the incoming polarization. The near-field nonlinear response is found to be directly related to local surface plasmon resonances and to particle morphology. The combined analysis of linear and SHG SNOM images provides discrimination among different light extinction/scattering particle behaviors, not achievable just with linear techniques.

I have spent the last year of my PhD in the Nano-Optics group in Zurich led by Prof. Sandoghdar, where I have developed a SCOM for the detection and spectroscopy of very small nanoparticles (diameter < 10 nm). By coupling into the SCOM and properly stabilizing a coherent source of white light, produced by spectral broadening in a photonic crystal fiber, it was possible to obtain extinction spectra of particles as small as 5 nm in diameter. On the other hand, thanks to an efficient referencing of a monochromatic green laser source, it was possible to dramatically increase the signal to noise ratio (SNR) of the system ($\text{SNR} > 10^4$); this improvement paved the way to the detection of single quantum emitters even in the absence of their fluorescence. The white light SCOM allows to measure the extinction spectrum

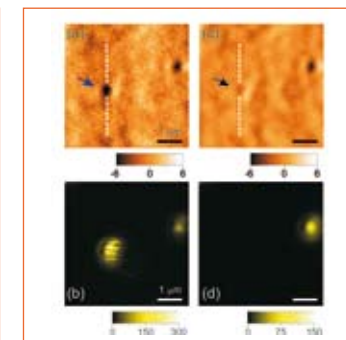
of a single metal nanoparticle, with diameter smaller than the electron mean free path (≈ 15 nm) thus gaining better insight into free electron motion in tightly confined clusters. Fig. 2(a) shows the extinction image of 5-nm diameter gold nanoparticles, while Fig. 2(c)



2. 5 nm gold nanoparticles. (a) a wide scan of an ensemble of single particles. Image is obtained by averaging the whole spectral response each pixel. (c) A spectrum of a single particle acquired while sitting on it; a strong blue-shift occurs with respect to 15-nm ones, that are comparable with electron mean free path (see panel b)

shows the extinction spectrum of a single 5-nm nanoparticle, which displays a significant blue-shift with respect to a 15-nm one (Fig. 2(b)). While spatial resolution of the SCOM turns out to be poor compared to that of the SNOM (compare Fig. 1 and 2a), its sensitivity is higher, allowing for efficient detection and spectroscopy of smaller nanoparticles. Finally, another exciting challenge in Nanooptics is the measurement of the weak light extinction which stems from single emitters. Through a substantial improvement on SCOM stability we were able to detect and image single nanocrystal quantum dots (i.e.

synthetic atoms) while they do not emit any light (bleaching state, see Fig. 3). This paved the way for a novel photophysical characterization of single quantum emitters.

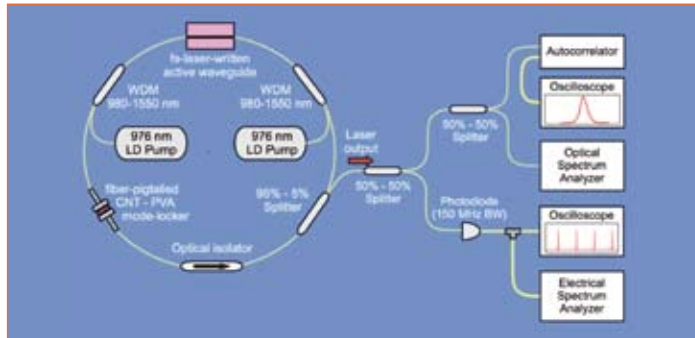


3. Detection of bleached dots. (a) extinction image of two quantum dots and (b) simultaneous fluorescence map. (c) and (d) same area imaged after the dot on the left has bleached

FEMTOSECOND LASER WRITING OF PHOTONIC COMPONENTS IN TRANSPARENT DIELECTRICS

Nicola Chiodo

Optical waveguides and related photonic devices, such as waveguide amplifiers and lasers, couplers, splitters, and interleavers, are finding increasing applications in optical communication systems. The integration on a single glass chip of several optical functions such as power splitting, wavelength multiplexing/demultiplexing and gain can enable all-optical data processing and provide reliable and cheap devices for high-bandwidth optical fiber links, especially for Local Area Network (LAN) and Metropolitan Area Network (MAN) applications. Traditional waveguide manufacturing technologies include chemical vapor deposition with subsequent reactive ion etching (silica on silicon), ion and sol-gel. While these techniques are well established, they present two main disadvantages: (i), they are multistep processes, including a photolithographic step limiting the flexibility of device fabrication; (ii) they are essentially two-dimensional techniques, capable of producing only structures in planar geometry close to the surface of the sample. Recently, a novel technique for the direct writing of waveguides and photonic circuits, exploiting refractive index modifications induced by focused femtosecond pulses, has emerged. The



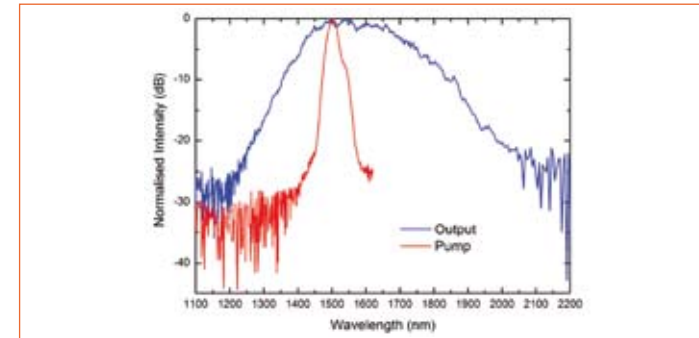
1. Scheme of the linear laser cavity setup employing a bi-directional pumping scheme. ISO: Optical Isolator. PC: Polarization Controller at $\lambda/2$

aim of my Ph. D. activity has been the modification of dielectrics to realize optical devices for applications in telecommunications using this technique.

The technique used to modify dielectrics consists on focusing a femtosecond laser beam on the on the surface, or below, of a transparent dielectric. The focused beam causes a local variation of the refractive index of the material; in the dielectrics in which that variation is positive there is the possibility to obtain waveguides with very good optical properties by moving the sample to respect the focus of the beam. The laser oscillator used to modify the dielectrics has as active material a crystal doped with ytterbium and is made by a laser cavity that works in mode-locking and generates pulses at a repetition

rate of 20 MHz. To increase the energy of the pulses and decrease repetition rate the cavity-dumper technique is used. That technique consists on Taking the pulse directly inside the cavity using an electro-optical modulator. To modify the material it is used the latter beam that is composed of pulses with duration of 300 fs, an energy of 1 μ J at arepetition rate variable between 400 kHz and 1.2 MHz.

With this technique we have realize active and passive optical devices. The active devices are: a waveguide laser working in mode-locking regime at a wavelength of 1550 nm that uses as active material a phospate glass doped with erbium and ytterbium. The waveguide has been manufactured with the femtosecond technique;



2. Graph showing supercontinuum and OPA pump spectra

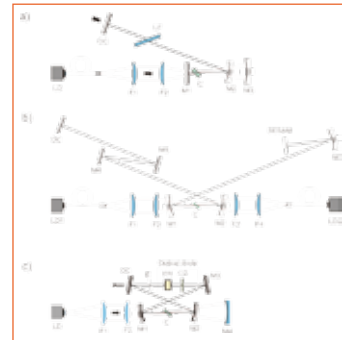
other waveguides lasers that use as active material a silicate glass doped with erbium and ytterbium and then a broadband optical amplifier manufactured in an innovative silica glass doped with bismuth. The passive devices are: a directional coupler in fused silica; an array of coupled curved waveguides to visualize Bloch oscillations; an optical device for generating second harmonic frequency in lithium niobate and and another for generating supercontinuum in a chalcogenide glass.

NEAR-INFRARED DIODE-PUMPED SOLID-STATE LASERS BASED ON FLUORIDE CRYSTALS

Nicola Coluccelli

Solid-state lasers with emission in the near and medium infrared find applications in various fields, from telecommunications to meteorology, from medicine to frequency metrology and high-resolution spectroscopy. In particular, lasers emitting around 1 and 2 μm are employed in LIDAR (*Light Detection and Ranging*) systems for environmental monitoring such as coherent Lidar-Doppler systems for wind velocity sensing, and DIAL (*Differential Absorption Lidar*) systems measuring the concentration of specific atmospheric components as water vapour (H_2O) and carbon dioxide (CO_2). In general, these systems are based on an oscillator with excellent power stability, high-spectral purity, and wide frequency tunability. All these features can be contemporary available in one laser source, employing stabilization techniques of the emission frequency on absorption lines of certain chemical compounds (CO_2 , H_2O , HBr), together with laser materials providing wide gain bandwidth. The aim of the PhD activity was the research and development of solid-state laser sources with emission around 1 and 2 μm , operating in both continuous-wave (cw) and pulsed regimes. A primary goal for cw sources is to demonstrate efficient and broadly tunable laser action. As regards to pulsed sources, the generation of ultra-short pulses in the 100-fs

regime is of great importance. The active materials investigated are Yb:YLiF₄, Yb:KYF₄, Tm:BaY₂F₈, and Tm:LiLuF₄ fluoride crystals. The pump sources employed in the developed lasers are laser diode arrays with maximum output power in the range from 3 to 5 W, and emission wavelengths of nearly 780 and 970 nm for Tm and Yb lasers, respectively. This choice for the pump sources leads to highly efficient and compact optical oscillators, with improved performance in terms of intensity and frequency noise, particularly suitable for LIDAR applications. A detailed study of the physics of rare-earth doped YLiF₄, KYF₄, BaY₂F₈, and LiLuF₄ fluoride crystals and an analysis of the energy levels of Yb³⁺ and Tm³⁺ doping ions are the necessary background for the experimental activity. Before performing laser experiments, the crystalline lattice structure, and the results of the spectroscopic measurements, specifically absorption and emission cross sections as well as upper laser level lifetimes, are examined for each of the above mentioned laser crystals. Once the absorption and emission cross sections are known, the gain cross sections, useful to predict laser performance, are calculated. Laser experiments were performed using various resonator configurations, depending on the different regimes of operation of the implemented lasers. The

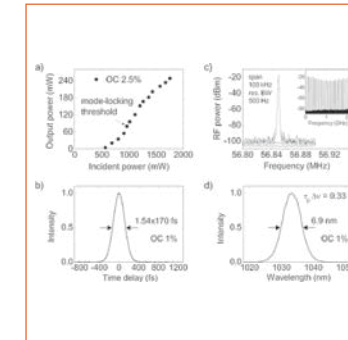


1. (a) V-shaped cavity; (b) X-shaped cavity; (c) Ring cavity. LD: laser diode; F: lens; M: mirror; OC: output coupler; LF: Lyot filter; C: active crystal; SESAM: saturable absorber mirror; E: etalon; FR: Faraday rotator; $\lambda/2$: half-wave plate

V-shaped cavity illustrated in [Fig.1 (a)] was adopted for cw laser experiments, and is designed to provide a tight intracavity focus and a nearly plane wave front inside one arm of the resonator, allowing low-loss insertion of optical elements such as birefringent filters, etalons, modulators. Mode-locking laser experiments were performed using the X-shaped cavity of [Fig.1 (b)], providing a tight intracavity focus of the modal beam leading to self-phase modulation (SPM) effects which broaden the spectra of the mode-locked laser field. Finally, implementation of the single-frequency Tm:BaY₂F₈ laser requires a unidirectional ring cavity to strongly reduce the number of oscillating modes. This resonator is illustrated in [Fig.1 (c)], and contains a Faraday rotator followed by a half-wave

plate acting as an optical diode to ensure unidirectional operation of the laser, and a high-finesse etalon to enforce single-mode longitudinal mode operation. The Yb:YLiF₄ laser was operated in cw and mode-locking regime. In cw regime, a maximum output power of 0.69 W at 4.3-W incident pump power and a slope efficiency of 22% were demonstrated, with wide wavelength tunability of the laser emission around 1 μm , ranging from 1010 to 1069 nm. The slope efficiency and tunability range represent the best results ever obtained with room-temperature Yb:YLiF₄ lasers. The first demonstration of passive mode-locking operation of an Yb-doped YLiF₄ crystal by means of saturable absorber mirrors (SESAM) is also reported. Pulse trains with minimum duration of 196 fs, 54-mW average power centered at 1028 nm and repetition rate of 55 MHz were obtained. Continuous-wave as well as mode-locking operation was also demonstrated using the Yb:KYF₄ crystal. During cw laser experiments, a maximum output power of 0.63 W and a slope efficiency of 36% were obtained with incident pump power of 2.2 W. The emission wavelength can be tuned over a 73-nm range, from 1012 to 1085 nm. This result represent the largest tunability ever demonstrated by Yb-doped fluoride crystals. As regards the mode-locking regime, it is reported the first demonstration of passive mode-locking of an Yb-doped KYF₄ crystal. A pulse duration of 170 fs with 8% optical slope efficiency was obtained. Among fluorides, Yb:KYF₄ generates pulses approaching the minimum pulse duration of 150 fs obtained with

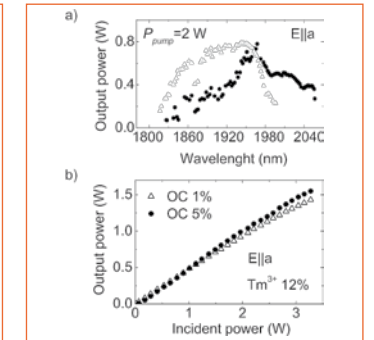
an Yb:CaF₂ laser (see [Fig. 2]). The cw emission properties of the Tm:BaY₂F₈ crystal for different Tm doping level, specifically 5%, 8%, and 12%, were examined. The best results were obtained with the 8% doped sample: a maximum output power of 1.01 W at 3.2-W incident pump



2. a) Average output power of the mode-locked Yb:KYF₄ laser; b) autocorrelation trace of the 170-fs duration pulses; c) RF spectrum of the fundamental harmonic of the pulse train; d) optical spectrum of the 170-fs duration pulses

power, and a slope efficiency of 43%. With the same 8% doped crystal, the widest tunability range of 245 nm, from 1780 to 2025 nm, was obtained. This is the largest tunability range ever demonstrated with a Tm-doped fluoride crystal. A Q-switched laser was also implemented using the Tm:BaY₂F₈ crystal. The highest energy of the output Q-switching pulses is 5.6 mJ, at a pulse repetition rate of 5 Hz, with pulse duration of 180 ns and peak power of 31 kW. The central wavelength of the pulses can be tuned from 1905 to 1990 nm. The results obtained with the Q-switched Tm:BaY₂F₈ laser operated at room temperature show a better slope efficiency and a wider tunability range compared with those reported for other Tm-doped bulk hosts.

Investigation of the cw laser emission properties of Tm:LiLuF₄ was performed for different Tm dopant ions concentrations (see [Fig. 3]). A maximum output power of 1.55 W at 3.4-W of incident pump power, a slope efficiency of 53%, and a remarkable wavelength tuning



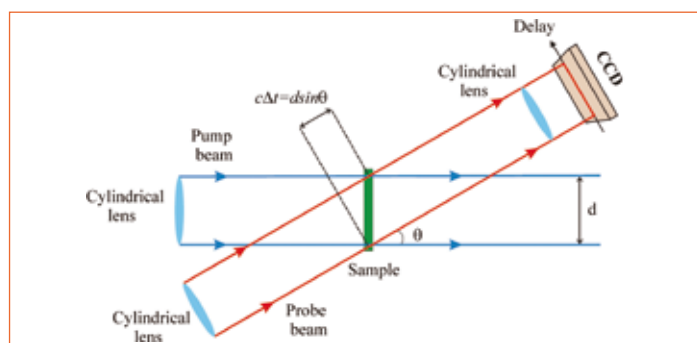
3. a) Tunability curve of the cw Tm:LiLuF₄ laser; b) cw output power of the Tm:LiLuF₄ laser

range of 230 nm, extending from 1826 to 2056 nm, were demonstrated with the optimized Tm concentration of 12%. Focusing on tunability range, output power, and slope efficiency, the results obtained with Tm:LiLuF₄ are comparable with the best results already demonstrated with several diode-pumped Tm-doped crystalline hosts. Among fluoride hosts, LiLuF₄ provides a tuning range that approaches the best result of 245 nm achieved with BaY₂F₈. Single-frequency operation is demonstrated using the Tm:LiLuF₄ crystal. A maximum output power of 120 mW, a slope efficiency of 13%, and a wavelength tuning range of 20 nm, from 1875 to 1895 nm, were demonstrated using a unidirectional ring resonator. The laser emission has high-spectral purity and a linewidth of 300 kHz over 1-ms observation time.

REAL-TIME PUMP-PROBE IMAGING SPECTROSCOPY

Raffaele Ferrari

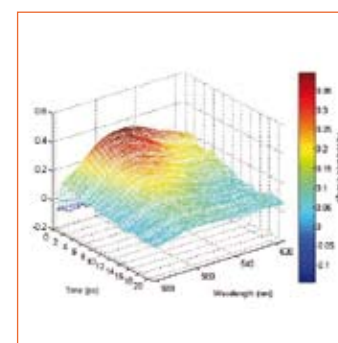
Over the past decades a considerable interest has been attracted by the study of photochemical and photophysical properties of many materials, in particular organic and biological. For example the study of light harvesting by carotenoids has conducted to a deeper understand of photosynthesis. However, organic and, in particular, biological materials are much more complex to be studied compared with inorganic because they easily deteriorate once exposed to light pulses, with the formation of permanent reaction products and structural changes. Moreover, the situation is often complicated by the small quantities of available biological sample. Pump-probe transient absorption spectroscopy is one of the most commonly used technique to study ultrafast phenomena. Generally, this technique requires a long acquisition time because temporal dynamics are obtained by repeating the measurement at different delays between the pump and probe beams. Hence, the possibility to have a technique which allows one to acquire a spectral transient absorption in real-time is fundamental to study irreversible processes such as the case of many biological samples or solids.



1. Schematic diagram of the technique

Recently, various real-time techniques have been proposed. Their basic idea is to encode time in space and to take advantage of bi-dimensional detectors, which have made a rapid progress in the last years. During my PhD, I studied a real-time pump-probe spectroscopy technique, I developed an instrumental set-up and I made measurements on samples of interest. In this technique, the spatially encoding of temporal information is realized through the non-collinear overlap of the pump and probe beams on the sample to investigate [Fig. 1]. Both beams are linearly focused by cylindrical lenses, and their focal lines spatially overlap on the sample. Since the pump beam incidence is normal, it reaches different parts of the sample at the same time. On the contrary, the probe beam arrives with an angle θ with respect

to the pump beam reaching different portions of the sample in different times. In this way a spatial encoding of the temporal information is realized. The width of the temporal interval Δt depends on geometrical parameters leading to a window of 4 ps. The laser pulses needed for the measurements are provided by a Ti:Sa oscillator followed by a regenerative amplification stage which generates pulses with 800 nm wavelength, 70 fs duration and 2 mJ energy. In addition, I used a white-light supercontinuum generated by a sapphire plate as probe and a second harmonic (400 nm) pump beam generated by a BBO crystal. Using a CCD sensor coupled to a spectrometer as detection device, also the spectral information in a band of wavelengths can be collected. It is worth noting that this



2. Frequency and time-resolved absorbance change in β -carotene solution

technique allows one to perform measurements with only a single laser pulse. However many samples require to average over many pulses because of the weakness of the signal. In addition the signal to noise ratio of the CCD can be a limit to the number of pulses needed for a measurement. I characterized the system by measuring ultrafast internal conversion of β -carotene, a carotenoid that has been extensively investigated through the conventional pump-probe transient absorption technique. A commercial powder of β -carotene dissolved in cyclohexane solution was measured. Adding 5 CCD frames, each covering 4 ps and each one acquired with 250 pulses, the map of photoinduced absorption changes in β -carotene can be measured [Fig. 2]. The spectral

and temporal information can be obtained by simply slicing off the map shown. This measurement has been repeated until 25 pulses per frame. In addition, the results have been compared with those obtained measuring the same sample with a conventional pump-probe system finding an optimum agreement.

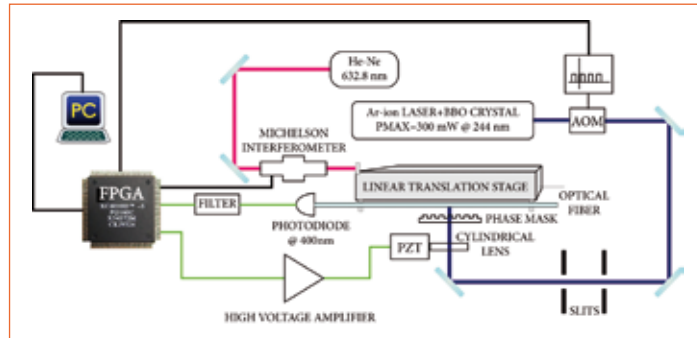
After that, I made measurements on polymeric samples which have a considerable interest in optoelectronic and which show often problems of degradation. First I studied a solution of poly-3-hexyl thiophene (P3HT) dissolved in chlorobenzene. P3HT is considered a promising candidate for high-efficiency photovoltaics because its ordered morphology enhances charge transport and mobility. Also in this case a map of the photoinduced absorbance change has been measured. The photodegradation caused by a long photoirradiation was also studied following the evolution of the transmission signal during the irradiation with the pump beam for many minutes. I obtained clear evidence of new absorbers species generated during the photoirradiation and of the presence of metastable energy levels with long lifetimes. Then I studied a sample constituted by a thin film of tetraphenylporphyrin doped

poly(9,9-dioctylfluorene) (PFO/TPP) where PFO, a blue emitting polymer, has been recently investigated for applications in efficient LEDs. The overlap between the emitting band of PFO and the absorption band of TPP makes efficient the process of Förster energy transfer, red-shifting the emission. I measured the photoinduced absorbance change of the blend, finding in particular the decay time of the signal at 780 nm where TPP has a negligible photoinduced signal. Repeating the same measurement after 10 minutes of irradiation of the sample, I found a shorter decay time. The irradiation has probably decreased the relative concentration of TPP in the blend making less efficient the Förster energy transfer.

FIBER BRAGG GRATINGS FOR TELECOMMUNICATION AND SENSING APPLICATIONS

Davide Gatti

Fiber Bragg gratings (FBGs) are passive optical devices obtained by a periodic or *quasi*-periodic weak modulation of the refractive index of an optical fiber core. The physical phenomenon responsible for the refractive index change after UV irradiation is called photosensitivity. FBGs are largely employed in optical communication field, as dispersion compensators, narrow band-pass filters, add-drop multiplexers and de-multiplexers in WDM (*Wavelength Division Multiplexing*) systems and more complex FBG design has enabled to perform advanced optical processing, such as pulse shaping, matched filtering and pulse compression. In the recent years the FBGs spreading in the sensing field has found several applications, ranging from *in situ* sensors in the medical industry for monitoring important biological functions, through to vast distributed sensors in the oil industry, up to the monitoring of the structural health of buildings, ships and aircraft. The aim of the PhD activity was the design, fabrication and characterization of FBGs with complex refractive index profiles for telecommunication and sensing applications. The first step to manufacture complex FBGs is to implement and validate a writing system allowing the realization of different index profiles. Three FBGs typologies



1. Grating writing setup. AOM: acousto-optic modulator; PZT: piezoelectric transducer

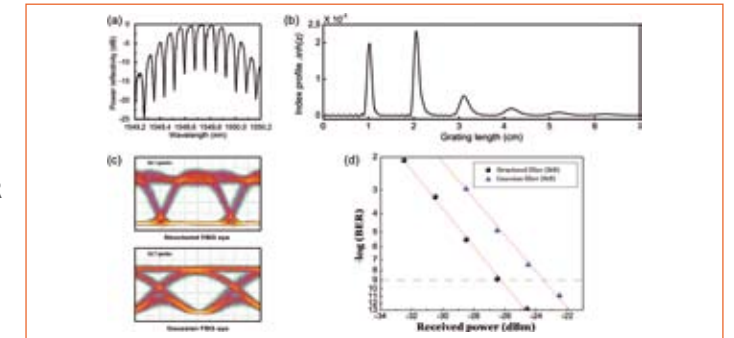
have been manufactured: the first is used as demodulator of DPSK (*differential-phase-shift-keying*) signals; the second represents an *optical buffer* based on the light slowing down, for all-optical signal processing; the third is a high-sensitivity dynamic strain sensor that may be employed as ultrasonic hydrophone in medical and geophysical applications. A theoretical analysis of different FBG characteristics, based on coupled-mode equations, is the fundamental starting point to understand the behaviour of such periodic structures. Bearing in mind the spectral response to be obtained, an inverse scattering algorithm is required: given the target spectral reflectivity it is possible to calculate the index profile of the FBG to synthesize. FBGs fabrication was performed using the experimental setup (based on the so called *continuous writing technique*)

displayed in [Fig. 1]. A UV beam leading out from a frequency-doubled Ar-ion laser, delivering about 200 mW at 244 nm of wavelength, is focused by a cylindrical lens into a fiber core and is strobed using an acousto-optic modulator. The phase mask is needed in order to generate an interference pattern responsible for the refractive index modulation. During the whole writing process the fiber is moved at constant speed and its position, synchronized with UV strobing to maintain the coherence between interference fringes, is accurately monitored by a Michelson interferometer with nanometric resolution. Such a system allows to realize FBGs up to 1 meter length with a nearly arbitrary index profile. Germanium doped fiber optics were chosen for their high photosensitivity. Every fiber is put in high-pressure hydrogen atmosphere, before the FBG

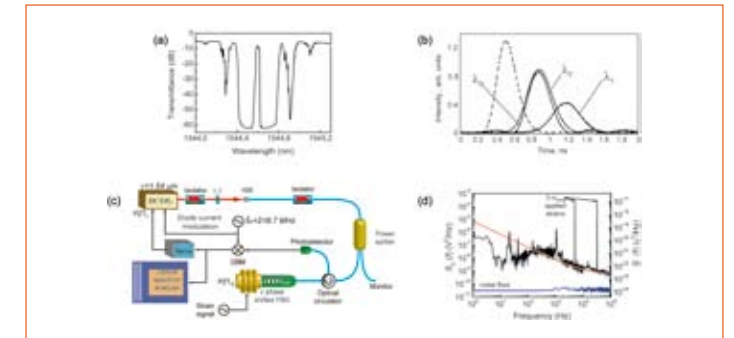
manufacturing, in order to enhance this phenomenon. We have synthesized and experimentally demonstrated an innovative structured FBG filter for optimal DPSK demodulation which is a valuable alternative to Mach-Zehnder (MZ) demodulators and current FBG-based filters. The filter was designed in order to mimic the MZ frequency response and to operate at the bit-rate of 10 Gbit/s. [Fig. 2] shows the spectral reflectivity (a), and the index profile of structured FBG (b), respectively. Eye-diagram and BER (*Bit error rate*) measurements, depicted in [Fig. 2], showed an error free transmission ($BER < 10^{-9}$) for a received power of -26.3 dBm, with an improvement of about 3 dB as compared with an optimized narrow Gaussian filter, which represents, at the state-of-the-art, the best alternative to MZ demodulator. The optical buffer is a key component of an all-optical processor and a superstructured FBG accomplishing this task has been realized; the possibility of slowing down the speed of light to almost one third of its vacuum value, exploiting transmission windows in the spectral response of superstructured fiber Bragg grating, has enabled the light pulse delay of its entire time duration, demonstrating the possibility to implement a fiber-based optical buffer. [Fig. 3] shows the transmission spectrum of the superstructured FBG (a), and pulse delay measurements (b), respectively. We notice that pulses travelling at the windows wavelength (solid lines) are slowed down with respect to a pulse propagating outside the FBG bandwidth (dotted line). The third FBG has been designed

to be employed as dynamic strain sensor with ultra-high sensitivity. Such kind of sensor is usually realized with piezoelectric actuators (PZT) which suffer from many drawbacks related to their electrical nature. The properties of a fiber-based device, like electromagnetic interference

narrow resonance is suitable to be used as frequency discriminator in a Pound-Drever-Hall (PDH) system. [Fig. 3(c)] shows the PDH experimental setup used in our experiments. The power spectral density of the voltage signal used to evaluate the device sensitivity, with respect to the frequency



2. (a) Power reflectivity and (b) refractive index profile of the FBG-based DPSK demodulator; (c) eye-diagrams and (d) BER measurement performed for both structured and Gaussian FBGs



3. (a) Transmittance of superstructured FBG and (b) pulse delay measurements; (c) PDH setup for dynamic strain detection and (d) power spectral density of the voltage signal at the output of double-balanced mixer (DBM) used to evaluate the strain sensitivity

immunity and passive operations, allows to overcome such problems with respect to PZTs. We have manufactured a uniform FBG with a π -phase-shift in its middle point. The narrow spectral transmission window, inside the FBG reflection bandwidth, has a FWHM (*full-width-at-half-maximum*) of 55 MHz. Such

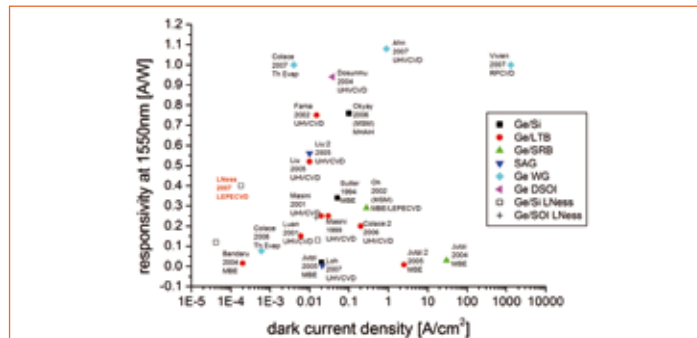
of the applied strain, is depicted in [Fig. 3(d)]. A piezoelectric actuator (PZT), glued to a FBG side, was used to calibrate the system (see the two peaks in figure). With this sensor, strains of the order of few picometers over one meter of fiber (in 1 Hz measurement bandwidth) have been detected for Fourier frequencies above 100 kHz.

MONOLITHICAL INTEGRATION OF Ge PHOTODIODES ONTO Si AND SOI SUBSTRATES

Johann Osmond

The demand for higher speed and lower costs in telecommunications drives a transition from electrical to optical. Silicon-based photonics seems to be the favorite solution to this transition as it could provide a full and monolithical integration of optics and electronics. It would also benefit from the large experience and facilities developed during the past for CMOS. Production costs would be lowered and technological processes simplified.

The actual solution in optoelectronics is hybrid integration. For example the photonics building block of photodetectors in the near infrared is actually dominated by III-V components which are however not compatible with Si integration. It requires moreover a complex fabrication, high cost hybridization and it introduces some losses which would be prevented by a monolithical integration of high speed photodetectors on Si platform. On the other hand SiGe alloys are a good alternative for detection in the telecommunications 1.2-1.6 μ m wavelength range due to their optical properties, to their full miscibility with Si and to their already proven compatibility with CMOS production. It makes the development of integration of Ge photodetectors



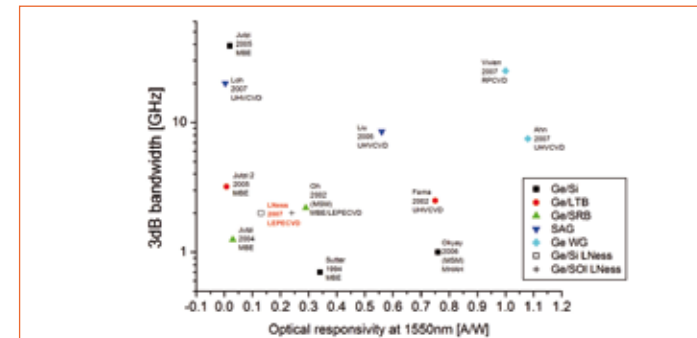
1. Plot of the performance of dark current at -1V bias and external optical responsivities at 1550nm of results published in literature and of significant results obtained in this work by LEPECVD grown material (empty black squares and black). All the photodiodes, except for the points indicated by Ge WG light blue diamonds, are top-illuminated

onto Si or SOI platform for optical communications highly attractive, as proved by the recently published achievements in this field by Luxtera and Intel companies.

A relatively new SiGe growth technique developed first in ETH Zürich (CH) and then in at the department of Physics of Politecnico di Milano in Como, the so-called Low Energy Plasma Enhanced Chemical Vapour Deposition (LEPECVD), showed excellent material properties and unique growth characteristics: high growth rate, independence of the deposition rates respect to substrate temperature and sharp control of the interfaces. This growth technique was then used to deposit Ge layers directly on Si and SOI substrates.

The Ge/Si heterojunctions were then processed as top illuminated p-i-n diodes and the performances of the obtained diodes (dark current density, optical sensitivity and 3dB bandwidth) were investigated and compared to the results published for other growth techniques.

The two figures in attachment resume the final results obtained for LEPECVD grown Ge heterojunctions and their comparison to literature. In [Fig. 1] we can see that the LEPECVD grown Ge photodiodes exhibit low dark current densities: comparable to reference values for highly doped samples on Si and SOI substrates and even the lowest ever reported for the low doped



2. Plot of the performance of external optical responsivities at 1550nm and 3dB bandwidth of results published in literature and of significant results obtained in this work by LEPECVD grown material (empty black squares and black cross). All the photodiodes, except for the points indicated by Ge WG light blue diamonds, are top-illuminated. The references of the results are the same as indicated in figure 1

samples. These results show the good quality of the material The photodiodes exhibit at the same time an acceptable but limited optical responsivity, which however could be improved by a better collection efficiency and an optimized antireflective coating. The optical responsivity value at 1550nm is always larger than 0.1A/W which is the limit required for an adequate receiver sensitivity. The bandwidth performance at 1550nm is moderate [Fig. 2] but it is most probably due to diode design or processing more than material quality.

The two figures of optical responsivity and bandwidth are expected to be largely improved by using waveguide integration

instead of top illumination configuration, as top illuminated photodetectors suffer from a trade-off between optical responsivity and bandwidth which is clearly visible in [Fig. 2]. On the other part waveguide integrated Ge photodiodes showed large values of the product of bandwidth by optical responsivities at 1550nm, as shown in [Fig. 2]. Preliminary studies of the realization of large width Si waveguides on SOI and of the integration of Ge vertically coupled photodetectors onto Si waveguides were finally realized.

HIGH RESOLUTION RIXS SPECTROSCOPY IN THE SOFT X-RAY RANGE: NEW INSTRUMENT AND RESULTS

Andrea Piazzalunga

The main activity of my PhD has been dedicated to the construction and first six months of operation of SAXES (Super Advanced X-ray Emission Spectrometer), a new innovative spectrometer for RIXS (Resonant Inelastic X-ray Scattering) and XES (X-ray Emission Spectroscopy) experiments. The instrument, designed for synchrotron radiation, operates in the soft x-ray (400-1,500 eV energy range), covering the O K edge, the 3d Transition metal $L_{2,3}$ edges and the $M_{4,5}$ edges of rare earths.

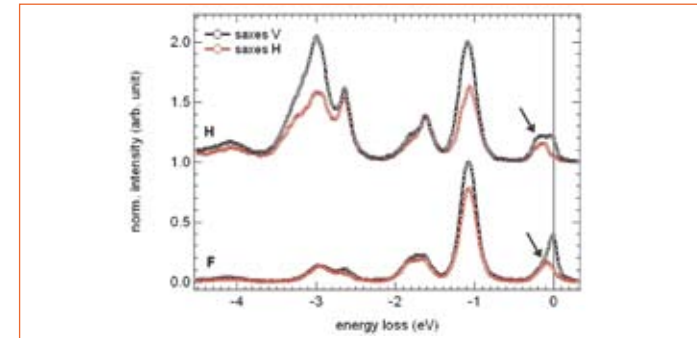
At present, SAXES is permanently installed on the ADDRESS (ADvanced REsonant Spectroscopies) beamline at the third generation synchrotron radiation SLS (Swiss Light Source), in Villigen (AG), Switzerland, where it is operating since July 2007. The main feature of the spectrometer consists in its extremely high resolution performances. A resolving power ($E/\Delta E$) better than 10,000 is reached over the whole operational range, i.e. considerably better than any other similar existing instrument. The spectrometer is 5 m long and is based on a VLS (variable line spacing) spherical grating with curvature radius $R=58.55$ m and average groove density of 3200 grooves/mm. It provides a flat field image on the surface of a position sensitive detector,



1.

consisting in a CCD (charge couple device) camera with $13.5 \times 13.5 \mu\text{m}$ pixel size. The whole spectrometer is installed on a rotating platform, allowing exploration of the scattering angle dependence (from 25° to 130°) and momentum transfer. The first year of my PhD has concerned the construction and first testing of the SAXES spectrometer [Fig. 1]. The instrument has been completely designed and built at the Physics Department of the Politecnico di Milano. In particular, my activity has consisted in the implementation and development of both mechanics and software parts of the spectrometer. A series of optics tests has been then performed in order to verify the correct working of the various mechanical components and the expected performances. The results have confirmed the good performances of

SAXES in terms of resolution and efficiency, allowing its future installation at the Swiss synchrotron SLS. For this reason, the whole spectrometer has been disassembled and installed at the ADDRESS beamline of the SLS, where I have permanently worked for one year and half of my PhD. There, the main subject of my activity has consisted in the remounting and implementation of the whole instrument, putting it in operation within the beamline environment. During this phase, I participate to the spectrometer and beamline commissioning, where I got practice with the various beamline instrumentations (undulator, monochromator and other optics elements). In the last six months of my PhD, various high resolution RIXS measurements have been performed with SAXES in a series of 3d transition



2.

metal compounds and rare earths systems. Within these measurements, I mainly concentrate on Nickel Oxide (NiO), which represents a well studied prototype of strongly correlated systems. A series of RIXS data have been acquired around the Ni L_3 edge (853 eV) for different scattering angle configurations of the spectrometer. One of the main results obtained from these measurements consists in the evidence of typical local spin-flip excitation features [Fig. 2], where by spin flip excitation is meant the transition involving a change in the orientation of the local spin moment on a Ni ion with respect to the orientation of other spin moments on neighboring Ni sites. Our measurements are of great importance since they represent the first direct experimental probe of such transitions with RIXS, thanks to the extremely

high resolution performances allowed by SAXES. Accurate RIXS calculations (using single atomic configuration and crystal field model), have accompanied the experimental measurements in order to perform precise assignments of the various spectral features and to obtain information on the various Hamiltonian parameters of the compound. In conclusion, the results of RIXS measurements on vanadium oxide (VO_2) performed at the ESRF (European Synchrotron Radiation Facility) in Grenoble (France), have been also considered. The accurate analysis of these data has allowed the determination of the various contributions to the spectrum, and, in particular, the main role of dd excitations. The information obtained on this compound could be useful for future theoretical investigations.

Thanks to:

Servizio Dottorati di Ricerca
Chairs and Secretaries of the Doctoral Programs
The Doctors of the Graduating Class of 2008

Graphic design and layout:

Bottega dei segni
www.bottegadeisegni.it

For further information:

www.polimi.it/phd
dottorato.ricerca@ceda.polimi.it

BIOENGINEERING | BUILDING ENGINEERING | DESIGN AND TECHNOLOGIES FOR CULTURAL HERITAGES | ELECTRICAL ENGINEERING | ENERGY | GEOMATICS AND INFRASTRUCTURES | INDUSTRIAL CHEMISTRY AND CHEMICAL ENGINEERING | INDUSTRIAL DESIGN AND MULTIMEDIA COMMUNICATION | INFORMATION AND COMMUNICATION TECHNOLOGY | INTERIOR DESIGN | MANAGEMENT, ECONOMICS AND INDUSTRIAL ENGINEERING | MANUFACTURING AND PRODUCTION SYSTEMS | MATERIALS ENGINEERING | MECHANICAL SYSTEMS ENGINEERING | **PHYSICS** | PRESERVATION OF ARCHITECTURAL HERITAGE | PROGRAMMING, MAINTENANCE, REHABILITATION OF THE BUILDING AND URBAN SYSTEMS | RADIATION SCIENCE AND TECHNOLOGY | SANITARY - ENVIRONMENTAL ENGINEERING | STRUCTURAL SEISMIC AND GEOTECHNICAL ENGINEERING | TECHNOLOGY AND DESIGN FOR ENVIRONMENTAL QUALITY IN BUILDINGS AND URBAN CONTEXT | URBAN AND ARCHITECTURAL DESIGN | URBAN PROJECTS AND POLICIES | URBAN, REGIONAL AND ENVIRONMENTAL PLANNING | VIRTUAL PROTOTYPES AND REAL PRODUCTS | WATER ENGINEERING | AEROSPACE ENGINEERING | APPLIED MATHEMATICS | ARCHITECTURAL COMPOSITION | ARCHITECTURE, URBAN DESIGN, CONSERVATION OF HOUSING AND LANDSCAPE